



ISSN: 0976-3376

Available Online at <http://www.journalajst.com>

ASIAN JOURNAL OF  
SCIENCE AND TECHNOLOGY

Asian Journal of Science and Technology  
Vol. 07, Issue, 08, pp.3473-3476, August, 2016

## RESEARCH ARTICLE

### STUDY OF GLCM FOR DIAGNOSIS OF LIVER DISEASES FROM ABDOMINAL CT IMAGES

**\*Suhaib Alameen and Mohamed E. M. Gar-Elnabi**

College of Medical Radiologic Science, Sudan University of Science and Technology,  
Khartoum, Sudan

#### ARTICLE INFO

##### Article History:

Received 25<sup>th</sup> May, 2016  
Received in revised form  
29<sup>th</sup> June, 2016  
Accepted 26<sup>th</sup> July, 2016  
Published online 30<sup>th</sup> August, 2016

##### Key words:

Classifications, GLCM,  
Liver Disease,  
Textural Features, CT.

#### ABSTRACT

In this paper we classify of liver diseases using Gray Level Co-occurrence Matrix (GLCM) to extract classification features from CT images. The techniques used here included Mean, variance, contrast, energy, entropy, correlation. To find the gray level variations in CT images, it complements the GLCM features extracted from CT images can be used to estimate the size distribution of the subpatterns. Linear discriminant analysis was used for the tissue classification. In This study found that the liver diseases texture reveals a different underlying pattern compared to the normal liver and other abdominal tissues with classification sensitivity and specificity 85.2% and 88.9% respectively, and the combination of the texture features throughout the different tri-phasic image phases provide the highest predictive. overall accuracy of 83.8 % using linear discriminant analysis. These relationships are stored in a Texture Dictionary that can be later used to automatically annotate new CT images with the appropriate organ names.

Copyright©2016, Suhaib Alameen and Mohamed E. M. Gar-Elnabi. This is an open access article distributed under the Creative Commons Attribution License, which permits unrestricted use, distribution, and reproduction in any medium, provided the original work is properly cited.

#### INTRODUCTION

The most familiar medical imaging studies for early identification of liver diseases comprise ultrasonography (US), computed tomography (CT), magnetic resonance imaging (MRI). CT is often the preferred method for diagnosing many different cancers than ultrasonography, since the image allows a physician to confirm the presence of a tumor and to measure its size, precise location and the extent of the tumor's involvement with other nearby tissue. Despite the excellence of CT images has been appreciably improved during the last years, it is hard in some cases, even for experienced doctors, to make a 100% precise diagnosis. In radiology computer-aided diagnosis (CAD) are procedures in medicine that help doctors in the analysis of medical images. CAD system can only provide a second opinion and cannot replace radiologists.

Focal liver lesions can be defined as any lesion in the liver other than the normal parenchyma with or without causing structural and functional abnormality of hepatobiliary system and can be of variable size. These lesions can be benign or malignant. Prevalence of various liver lesions has marked differences across geographic regions and ethnic groups.<sup>1</sup> Focal liver lesion is more likely to represent a metastatic deposit than primary malignancy in Europe and United States; however, hepatocellular carcinoma is the fourth most common hepatic disorder in Pakistan with prevalence of 8-10%. This prevalence rate is high when compared to western data.<sup>2,3</sup>

It is often difficult to characterize hepatic lesions with various imaging studies. Although histopathology is the gold standard, biopsy is always not possible as it is an invasive technique. Computed tomography (CT) is the imaging modality most often used to evaluate focal liver lesions, however, the complex blood supply of the liver frustrates the search for an optimal contrast-enhanced CT protocol for the detection and characterization of focal hepatic lesions. Although the liver receives approximately 30% of its blood supply from the hepatic artery and 70% from the portal vein, most primary and secondary liver neoplasms receive 80-95% of their blood supply from the hepatic artery. Because of the high frequency of benign focal liver lesions such as cysts, haemangiomas and focal nodular hyperplasia, characterization of these lesions is essential. Consequently, the preferred liver CT technique should combine a high sensitivity for lesion detection with a good ability for lesion characterization, to differentiate lesions that do need further diagnostic tests or treatment for lesions that do not. To meet these requirements, a triphasic spiral CT technique was developed to image the entire liver in arterial, portal, and equilibrium phases.<sup>4,5</sup> Although current literature search shows that MRI has a comparable rate in detection and classification of focal liver lesions, however, rapid availability and short scanning time made CT an ideal imaging technique.<sup>6-7</sup> Recent studies have also reported an improvement in lesion detection if arterial phase imaging is performed in addition to

portal venous imaging especially in the presence of hypervascular neoplasms, such as hepatocellular carcinoma.<sup>9-11</sup>

### Texture measure features and techniques

Several textural analysis techniques have been proposed to extract useful features for reliable liver tissue classification. Some extensively used techniques are:

- Gray Level Difference Statistics (GLDS): GLDS is the Probability Density Function (PDF) of pair pixels lying at specific distance and having a particular intensity value difference. Inter pixel gray level values have large variation for fine texture and least variation for coarse texture.
- Spatial Gray level Dependence Matrices (SGLDM): SGLDM [1] exploits the fact that spatial relationship between gray levels of an image contributes to overall texture properties of the image. It computes matrix by counting how many times pixels with intensity  $i$  and  $j$  occur at specified offset.
- Gray level Run length Statistics (RUNL): RUNL [2] makes use of the fact that there are consecutive points in image having same gray level along a particular direction. Coarse texture contains relatively long runs than short runs. Opposite is true for fine texture.
- Gray Level Histogram: It employs intensity distribution of image to find out texture parameters.
- Edge Frequency based Texture Features: These features are inversely related to the autocorrelation function and are based on distance related gradient. Micro-edges and macro-edges can be detected using small and large distance operator respectively.

### The Grey Level Co-occurrence Matrix for texture characterization

The Grey Level Co-occurrence Matrix (GLCM) is a pixel-based well known statistic used for texture analysis, because it provides some information like the texture contrast, homogeneity, entropy, energy, and correlation. It computes, for each possible pair of grey levels ( $g_1, g_2$ ), the number of pairs of pixels, having intensities  $g_1$  and  $g_2$ , which are situated from each other at a distance given by a specified displacement vector ( $dx, dy$ ). In practice, the GLCM probability is used, in order to scale the result:

$$p(g_1, g_2) = \frac{C_D(g_1, g_2)}{\sum_{g_1, g_2} C_D(g_1, g_2)}$$

The most relevant second order statistics computed using GLCM, which reveal important properties of the texture, are:

#### Contrast:

$$Contrast = \sum_i \sum_j (i - j)^2 p(i, j)$$

#### Total Energy (The angular second moment)

$$Total\_Energy = \sum_{i,j} (p(i, j))^2$$

#### Entropy

$$Entropy = \sum_{i,j} p(i, j) \log p(i, j)$$

#### Variance

where  $\mu$  is the GLCM mean.

$$Variance = \sum_i \sum_j (i - \mu)^2 p(i, j)$$

#### Correlation

$$Correlation = \frac{\sum_i \sum_j (i - \mu_x)(j - \mu_y) p(i, j)}{\sigma_x \sigma_y}$$

Where  $\mu_x$  and  $\mu_y$  are the GLCM mean after the first, respectively the second component and  $\sigma_x$  and  $\sigma_y$  are the GLCM variances after the first, respectively the second component.

### Data based acquisition

All patients examined on a Helical Multi detector CT scanner scanner (Somatom Siemens scanner dual slice, Asteion, TX-021B Toshiba scanner 16 slice, Philips Brilliance 64 slice and Aquilion, CXXG-012A Toshiba scanner 64 slice), used for collecting data from CT Abdominal images. With 8 second rotation Time, Large SFOV, 120 kVp and 320 mAs which differ through the phases. The protocol used for Abdomen scanning triple-phase helical CT with KVP of 120 and 250 and 320 mAs, slice thickness is depending on the structure being scanned, thin data require slice thickness of 5mm for reformatted images.

### Technique

Images from 180 patients was gathered. The acquisitions were performed with MDCT device and the standardized acquisition protocol was applied: helical scanning, with slice thickness 5 mm for each patient, an appropriate amount of 60% Iodinated Contrast material (about 100 -150 ml), was injected at 4 ml/s rate. The acquisition of the images in the arterial phase started about 20 seconds after contrast injection. Images corresponding to the portal phase were acquired with delay of 50–60s sequences with single Breath-holds. All images had a size of 512×512 pixels with 8-bit gray levels and were represented in DICOM format.

## RESULTS AND DISCUSSION

In this paper were features extracted from CT images using GLCM. and this features showed significant correlation with the predefined classes (Disease Liver, Normal Liver, Bone and Ribs) they included Mean, variance, contrast, energy, entropy, correlation. All these feature were calculated for all images and then the data were ready for discrimination which was performed using step-wise technique in order to select the most significant feature that can be used to classify the HCC in tri-phasic CT imaging and the results show that:

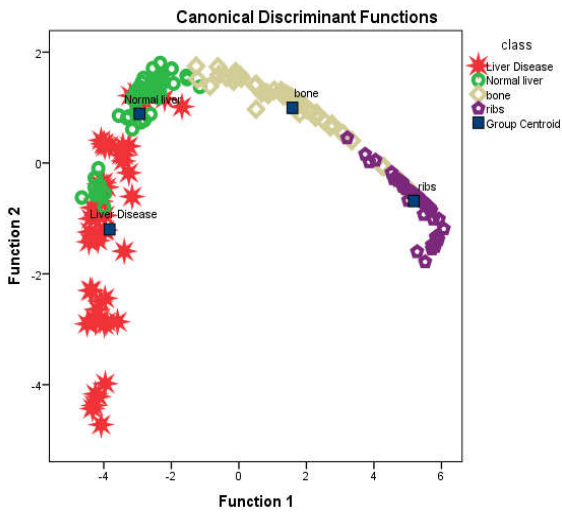


**Fig. 1. Scatter plot generated using discriminate analysis function for four classes represents:, liver disease, normal liver, bone and ribs**

The features of the classified regions of the whole images (as raw data) were classified further using linear discriminant analysis.

**Table 1. Showed the classification accuracy of the liver disease using linear discriminant analysis**

Classes	Predicted Group Membership				Total	
	Liver Disease	Normal Liver	Bone	Ribs		
Original	Liver Disease	85.2	33.3	1.9	.0	100.0
	Normal Liver	11.1	88.9	.0	.0	100.0
	Bone	.0	.0	66.7	33.3	100.0
	Ribs	.0	.0	5.6	94.4	100.0

83.8% of original grouped cases correctly classified

Table (1) show classification score matrix generated by linear discriminant analysis and classification accuracy of 83.8%. The classification accuracy of liver disease 85.2 %, normal liver accuracy 88.9 %, While the bone and ribs showed a classification accuracy of 66.7, 94.4 % respectively.

**Error bar plot for the CI Mean textural features**

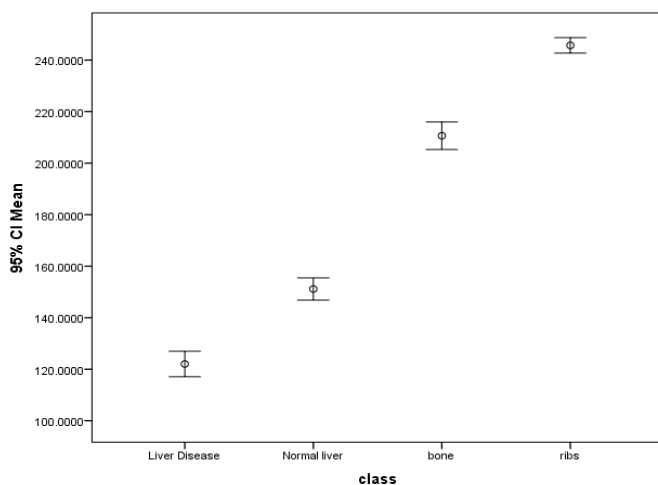


Figure (2) show error bar plot for the CI Mean textural features that selected by the linear stepwise discriminant function as a discriminate feature where it discriminate between all features. From the discriminate power point of

view in respect to the applied features the mean can differentiate between all the classes successfully.

**Error bar plot for the CI IDM textural features**

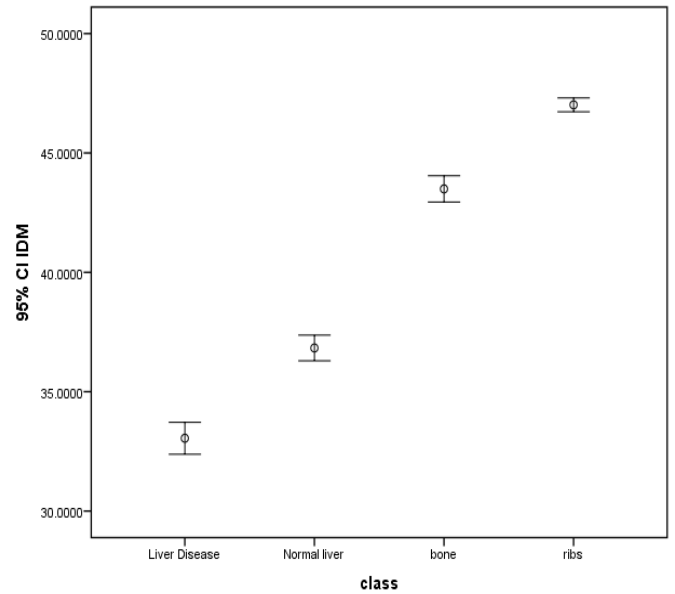


Figure (3) show error bar plot for the CI IDM textural features that selected by the linear stepwise discriminant function as a discriminate feature where it discriminate between all features.

**Error bar plot for the CI entropy textural features**

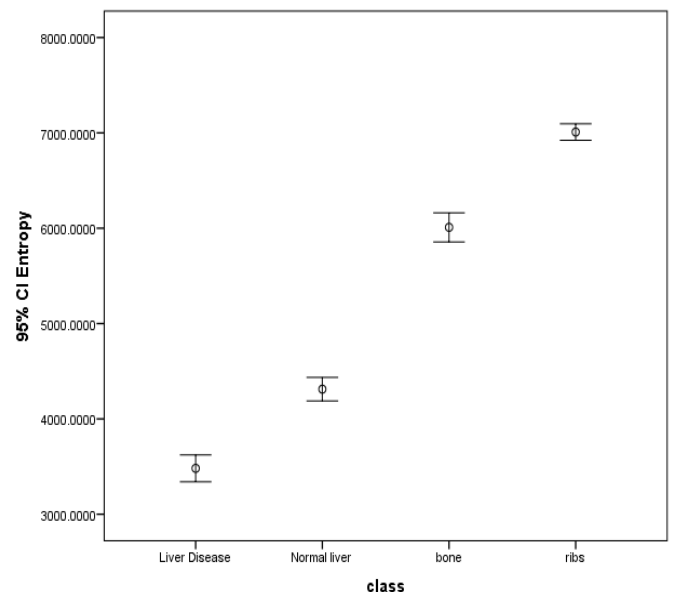


Figure (4) show error bar plot for the CI entropy textural features that selected by the linear stepwise discriminant

function as a discriminant feature where it discriminates between all features.

## Conclusion

The classification of regions in CT Abdomen were defined liver disease, normal liver, bone and ribs and the features of the classified regions of the whole images as raw data were classified further using linear discriminant analysis. The classification processes were carried out using Interactive Data Language (IDL) program as platform for the generated codes. The result of the classification showed that the liver disease areas were classified well from the rest of the tissues although it has characteristics mostly similar to surrounding tissues. Using Linear Discrimination Analysis generated a classification function which can be used to classify other image into the mentioned classes as using the following multi-regression equation; where the vote will be for the class with a higher classification score

$$\text{Liver Disease} = (\text{Mean} * 680.508) + (\text{IDM} * -5275.470) + (\text{entropy} * 5786.405) - 22306.152$$

$$\text{Normal Liver} = (\text{Mean} * 679.860) + (\text{IDM} * -5269.056) + (\text{entropy} * 5785.504) - 22304.197$$

$$\text{Bone} = (\text{Mean} * 681.278) + (\text{IDM} * -5278.841) + (\text{entropy} * 5789.992) - 22312.293$$

$$\text{Ribs} = (\text{Mean} * 683.005) + (\text{IDM} * -5292.097) + (\text{entropy} * 5792.124) - 22310.872$$

In conclusion the applied algorithm showed a potential success to adopt such procedure in medical image processing.

## REFERENCES

- Bonaldi, V.M., Bret, P.M., Reinhold, C., Atri, M. 1995. Helical computed tomogram of liver, value of an early hepatic arterial phase *Radiology*, 1995; 197: 357-63.
- Francis, I.R., Cohan, R.H., McNulty, N.J., Platt, J.F., Korobkin, M., Gebremariam, A, et al. 2003. Multidetector CT of the liver and hepatic neoplasms: Effect of multiphase imaging on tumor conspicuity and vascular enhancement. *AJR Am J Roentgenol*, 180: 1217-24.
- Hammerstingl, R., Huppertz, A., Breuer, J., Balzer, T., Blakeborough, A., Carter, R. et al. 2008. Diagnostic efficacy of gadoteric acid (Primovist)-enhanced MRI and spiral CT for a therapeutic strategy: comparison with Intraoperative and histopathologic findings in focal liver lesions. *EurRadiol*, 18:457-67.
- Iannaccone, R., Piacentini, F., Murakami, T., Paradis, V., Belghiti, J., Hori, M. et al. 2007. Hepatocellular carcinoma in patients with non-alcoholic fatty liver disease: helical CT and MR imaging findings with clinical-pathologic comparison. *Radiology*, 243: 422-30.
- Ichikawa, T., Saito, K., Yoshioka, N., Tanimoto, A., Gokan, T., Takehara, Y, et al. 2010. Detection and characterization of focal liver lesions: a Japanese phase III, multicenter comparison between gadoteric acid disodium enhanced magnetic resonance imaging and contrast enhanced computed tomography predominantly in patients with hepatocellular carcinoma and chronic liver disease. *Invest Radiol* 2010; 45: 133-41.
- Javed, I.F., Rukhsana, J.F. 2000. Prevalence of hepatocellular carcinoma in Pakistan in liver cirrhosis: An experience in NWFP. *J Coll Physicians Surg Pak*, 2:54-5.
- Méndez-Sánchez, N., Villa, A.R., Chávez-Tapia, N.C., Ponciano-Rodríguez, G., Almeda-Valdés, P., González, D. et al. 2005. Trends in liver disease prevalence in Mexico from 2005 to 2050 through mortality data. *Annals of Hepatology*, 4: 52-5.
- Soyer, P., Sirol, M., Fargeaudou, Y., Duchat, F., Hamzi, L., Boudiaf, M., et al. 2010. Differentiation between true focal liver lesions and pseudolesions in patients with fatty liver: evaluation of helical CT criteria. *EurRadiol*, 20: 1726-37.
- Szklaruk, J., Silverman, P.M., Chamsangavej, C. 2003. Imaging in the diagnosis, staging, treatment and surveillance of hepatocellular carcinoma. *AJR Am J Roentgenol*, 180: 441-54.
- Van Leeuwen, M.S., Noordzij, J., Feldberg, M.A., Hennipman, A.H., Doorneewaard, H. 1996. Focal Liver lesions; characterization with triphasic computed tomography *Radiology*, 201: 327-36.
- Yaqoob, J., Bari, V., Usman, M. U., Munir, K., Mosharaf, F., Akhtar, W. 2004. The evaluation of hepatocellular carcinoma with biphasic contrast enhanced helical computed tomography, *scan J Pak Med Assoc* 2004; 54: 123-7.

\*\*\*\*\*